Atomic Number Fluctuations in Spinor Bose–Einstein Condensate with Dynamical Quantum Phase Transitions

Yaming Li, Yi Ding, Jianning Liu and Yixiao Huang*

School of Science, Zhejiang University of Science and Technology, Hangzhou, 310023, China

Received: 06.08.2022 & Accepted: 7.11.2022

Doi: 10.12693/APhysPolA.143.83 *e-mail: yxhuang@zust.edu.cn

We study atomic number fluctuations in a spinor Bose–Einstein condensate and use it to characterize behaviors of dynamical quantum phase transitions. We observe that the quench dynamics of the atomic number fluctuations exhibit a nonanalytical change with respect to a parameter in the final Hamiltonian and demonstrate that the atomic number fluctuations can be used to detect both the ground state phase diagram and the highest energy state quantum phase transition. We further analyze the dynamics of atomic number fluctuations for finite magnetization and show that the quantum fluctuations could also be used to probe the phase transitions of the highest energy level and the ground state.

topics: atomic number fluctuations, spinor Bose–Einstein condensate, dynamical quantum phase transitions

1. Introduction

In recent years, nonequilibrium quantum many-body dynamics have attracted significant interest and seen rapid progress due to experimental technology advances in various physical systems, such as trapped ions [1, 2], Rydberg atoms [3], and ultracold atoms [4–6]. A most important question in this field is dynamical quantum phase transition (DQPT), which usually arises when the quench dynamics undergo a nonanalytic change with respect to a system parameter in a quenched Hamiltonian of the system [2–6]. Generally, the DQPTs are closely related to the quantum phase transition of the ground state. However, it was shown that the DQPT with no correspondence in the ground state quantum phase transition was related to an excited state phase diagram that may occur [7–11].

Spin-1 Bose–Einstein condensate is an ideal platform to study the nonequilibrium dynamics. The spinor condensate shows many interesting phenomena, such as topological defects [12–16], spin domains [17–21], the quantum Kibble–Zurek mechanism [22–31], and DQPTs. The DQPTs were observed in the recent spinor condensate experiment [32, 33]. It showed that the DQPTs not only reflect the ground phase transitions [32] but also correspond to an excited state phase transition [33]. In the previous works, the DQPTs were usually signaled by measuring the fractional population in the spin-m_f component. However, the DQPTs may be related to quantum fluctuations, which have a close relation to quantum metrology [34–51].

In this paper, we investigate the dynamics of the atomic number fluctuations and the DQPTs in a spin-1 condensate. We show that atomic number fluctuations can be used to describe the behaviors of the DQPTs. We find that the dynamical behaviors of the atomic number fluctuations reflect both the ground state phase transition and the phase transition for the highest energy level. Starting an initial state with all of the atoms equally condensed in the $m_F = \pm 1$ modes, we find the quench dynamics of atomic number fluctuations exhibit sudden changes at two critical points of the quadratic Zeeman energy, which correspond to the ground state and the highest energy level phase transitions, respectively. We investigate the quantum Fisher information of the state generated by the spin mixing dynamics and show that the optimal quantum Fisher information attains a Heisenberg scaling of the metrological sensitivity with N^2. We further investigate the quantum phase transition with nonzero spin magnetization m_z and show that the dynamics of the atomic number fluctuations characterize the ground state and the excited state phase transitions with nonzero m_z.

2. Atomic number fluctuations in a spinor condensate

We consider a system of spin-1 Bose–Einstein condensate with an external magnetic field, which has been realized in the experiment with ^{23}Na (or ^{87}Rb) atoms [52–54]. For both ^{23}Na and ^{87}Rb atoms, the spin-dependent interactions are typically

much smaller than the spin-independent ones. In such a case, we can use the single-spatial-mode approximation, which allows us to decompose the atomic field operator as $\hat{\psi}_m(r) = \hat{a}_m\phi(r)$ with $\hat{a}_m$ being an annihilation operator of the mth spin mode and $\phi(r)$ being a spin-independent mode function. Under the single-spatial-mode approximation, the Hamiltonian of the system takes the form [55, 56]

$$\hat{H} = \frac{c_2}{2N}\hat{\boldsymbol{S}}^2 + \sum_{m_f=-1}^{1}\Big(q\,m_f^2 - p\,m_f\Big)\hat{a}^\dagger_{m_f}\hat{a}_{m_f}, \tag{1}$$

where $\hat{\boldsymbol{S}}$ is the total angular momentum operator, N is the total particle number of the system, $m_f = -1, 0, 1$ being the magnetic spin quantum number, q and p correspond to the quadratic and linear Zeeman energy shift, respectively. The parameter c_2 is the spin-dependent interaction energy, and $c_2 < 0$ and $c_2 > 0$ correspond to the ferromagnetic and antiferromagnetic, respectively. Here, we notice that the term of the magnetization $\hat{S}_z = \hat{a}_1^\dagger\hat{a}_1 - \hat{a}_{-1}^\dagger\hat{a}_{-1}$ commutes with all the other terms in the Hamiltonian. If we consider the initial state of the system an eigenstate of $\hat{S}_z$, the dynamical evolution is restricted in the subspace of $\hat{S}_z$, and thus we can neglect the linear Zeeman term. In this work, all the atoms have been initially prepared in the $m_f = \pm 1$ modes, i.e., $|N/2, N/2, 0\rangle$. In the so-called 'pairs' basis $|N, k\rangle$, where N is the total particle number and k is the number of pairs of atoms in the $m_F = \pm 1$ states, it is convenient to write the above initial state as $|N, 0\rangle$. The effective Hamiltonian in such a subspace becomes

$$\hat{H} = \frac{c_2}{2N}\hat{\boldsymbol{S}}^2 - q\,\hat{a}_0^\dagger\hat{a}_0. \tag{2}$$

The Hamiltonian exhibits different phases by tuning the value of the quadratic Zeeman effect q and the spin-dependent collision interaction c_2.

In Fig. 1, we plot the atoms in the $m_f = 0$ mode, $\mathcal{N}_0 \equiv \langle\hat{N}_0\rangle/N$, of the ground state and the highest energy state for different q/c_2 with $c_2/h = 15$ Hz, which corresponds to the case of antiferromagnetic. As shown in Fig. 1a, the ground state exhibits a phase transition at $q = 0$. When $q > 0$, the ground state is a polar phase with all atoms occupying the $m_f = 0$ mode, while when $q < 0$, the ground state is an antiferromagnetic (AFM) phase with equally populated atoms in the $m_f = \pm 1$ modes. In Fig. 1b, the highest energy state shows a phase transition at $q = -2c_2$. When $q < -2c_2$, the state is a polar phase, while when $-2c_2 < q < 2c_2$, the state is a broken axisymmetry (BA) phase with a nonzero population in the $m_f = 0$ mode. When $q > 2c_2$, the highest energy state is an AFM state.

Next, we study the dynamical property of the system and discuss DQPT. To study the spin-mixing dynamics, we tune the quadratic Zeeman energy q in the dynamical process. The quadratic Zeeman effect q can be tuned by controlling a magnetic field and a microwave pulse, i.e., $q = q_M + q_B$, where q_B and q_M correspond to the quadratic Zeeman energy induced by a magnetic field and a microwave dressing field, respectively. For the spinor condensate, Zeeman energy q_B is always positive, while q_M can be swept from $-\infty$ to $+\infty$ in the current experiment [57].

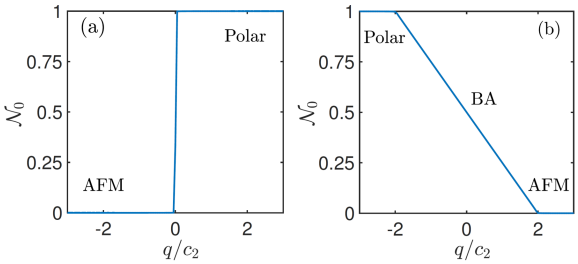

Fig. 1. The order parameter $\mathcal{N}_0$ for the ground state (a) and the highest energy level (b) as a function of q/c_2 with the total atom number $N = 2 \times 10^3$. The same phase diagrams were shown in [33].

We prepare the initial state to be the AFM state, where all of the atoms are condensed in the $m_f = \pm 1$ modes. Such an initial state can be generated by setting the initial quadratic Zeeman energy $q_i \to -\infty$. We then quickly turn on a microwave dressing field and lead the quadratic Zeeman energy to the final q_f. Then we hold the system at q_f for a given time t and then measure the fractional populations in the $m_f = 0$ mode and the corresponding quantum fluctuation, $\Delta\hat{N}_0^2 = \langle\hat{N}_0^2\rangle - \langle\hat{N}_0\rangle^2$. In Fig. 2, we plot $\mathcal{N}_0$ and $\Delta\hat{N}_0^2$ as a function of t for different q_f. It clearly shows that $\mathcal{N}_0$ and $\Delta\hat{N}_0^2$ exhibit different behaviors for different q_f. When $q_f > 2c_2$ and $q_f < 0$, $\mathcal{N}_0$ and $\Delta\hat{N}_0^2$ exhibit periodic oscillations over time. While $q_f = 0$ or $q_f = 0.5c_2$, we find that the phenomena of periodic oscillations disappear.

3. Signatures of dynamical quantum phase transitions

Generally, a dynamical phase transition is described by an asymptotic longtime steady value of an order parameter which can be described as $\langle\bar{O}\rangle_\infty = \lim_\infty \frac{1}{T}\int_0^T \mathrm{d}t\,\bar{O}(t)$. However, it is difficult to measure the quantity $\langle\bar{O}\rangle_\infty$ in the practical experiment because it requires averaging over a long evolution time t. For our system, several challenges will inevitably appear for a long evolution time t, such as invalidity of the single mode approximation (SMA) and significant atom losses [22, 58, 50], which prevent the practical observations of DQPTs.

Here we propose to identify DQPTs using the quantum fluctuation $\Delta\hat{N}_0^2$, which can be directly measured within short-time evolutions and has a close relation to quantum metrology. We define a quantity $\Delta\mathcal{N}_m$ being the value of $\Delta\hat{N}_0^2$ at the first peak of the fluctuation oscillations and denote the corresponding time of the occurrence of the first peak as t_m. Similarly, we define the particle

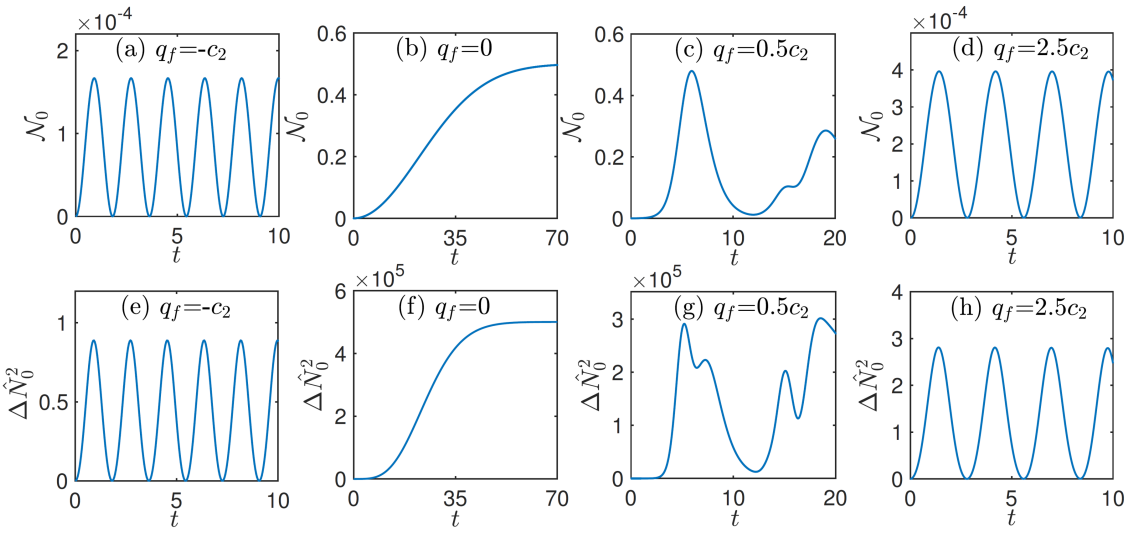

Fig. 2. The fractional populations $\mathcal{N}_0$ (a–d) and the atomic number fluctuations $\Delta\hat{N}_0^2$ (e–h) as a function of t starting with an initial state $|N/2, N/2, 0\rangle$ for different q. The total particle number is chosen as $N = 2\times10^3$.

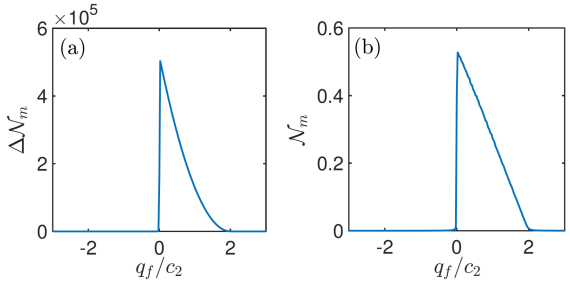

Fig. 3. The quantum fluctuation $\Delta\mathcal{N}_m$ (a) and $\mathcal{N}_m$ (b) as a function of q_f/c_2 with the initial state $|N/2, N/2, 0\rangle$. The total particle number is chosen as $N = 2\times10^3$.

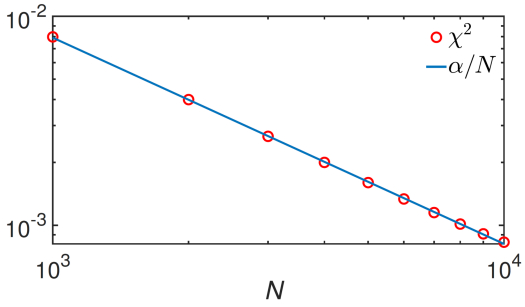

Fig. 4. Scaling of χ^2 as a function of N with the initial state $|N/2, N/2, 0\rangle$. The circles are numerical results, while the solid blue line is a linear fit with N a constant. It is obvious that $\chi^2 \propto 8/N$.

number in the $m_f = 0$ mode at t_m as $\mathcal{N}_m$. As shown in Fig. 3, $\Delta\mathcal{N}_m$ and $\mathcal{N}_m$ are plotted as a function of q_f/c_2. We find that $\Delta\mathcal{N}_m$ and $\mathcal{N}_m$ exhibit different behaviors in different regions of q_f and display nonanalytic sudden jump at exactly the same q_f as that shown in Fig. 1. It indicates that the dynamical behaviors of $\Delta\mathcal{N}_m$ and $\mathcal{N}_m$ can be used to probe DQPTs.

For a quantum state $\hat{\rho}_\theta = \hat{U}_\theta\hat{\rho}_{\text{in}}\hat{U}_\theta$, where $\hat{U}_\theta = \exp(\mathrm{i}\theta\hat{K})$ with $\hat{K}$ being an operator. The parameter θ can be estimated through proper measurements. It is well known that the precision of the estimation is limited by the quantum Cramér–Rao bound, i.e., $\Delta\theta \geqslant 1/\sqrt{F(\hat{\rho}_{\text{in}}, \hat{K})}$, where $F(\hat{\rho}_{\text{in}}, \hat{K})$ is the quantum Fisher information. For pure states, we have $F(\hat{\rho}_{\text{in}}, \hat{K}) = 4\Delta\hat{K}^2$. Obviously, the precision of the estimation can be improved by choosing a proper input state $\hat{\rho}_{\text{in}}$ for a given operator $\hat{K}$. In general, the entangled states are useful for the precision of the estimation because the corresponding variance of $\hat{K}$ is large. Here we choose a single generator to consider — $\hat{K} = \hat{N}_0$. In Fig. 3, we find that when $q_f = 0$, $\Delta\mathcal{N}_m$ attains its maximum value. For the spin-1 system, the maximal possible value of the quantum Fisher information is $4N^2$, which corresponds to the Heisenberg limit. To investigate the precision of the sensitivity, in Fig. 4, we plot the scaling of $\chi^2 = 4N/F$ as a function of N with $q_f = 0$. We find $\chi^2 \propto 8/N$, which means it is close to the Heisenberg limit.

Next, we discuss the phase transition for a finite spin magnetization m_z. In Fig. 5a and b, the ground state and the highest energy level phase diagrams are mapped out in the plane of q and m_z, respectively. When m_z rises from 0, the critical points for the ground state phase transition slightly increase from 0, and for the highest energy level slightly decreases from $2c_2$. Unlike in the case of $m_z = 0$ for the ground state, we find the BA phase appears with nonzero m_z (see Fig. 5a).

Now we study the DQPT with a nonzero spin magnetization. We prepare a state corresponding to an AFM phase with a large negative q,

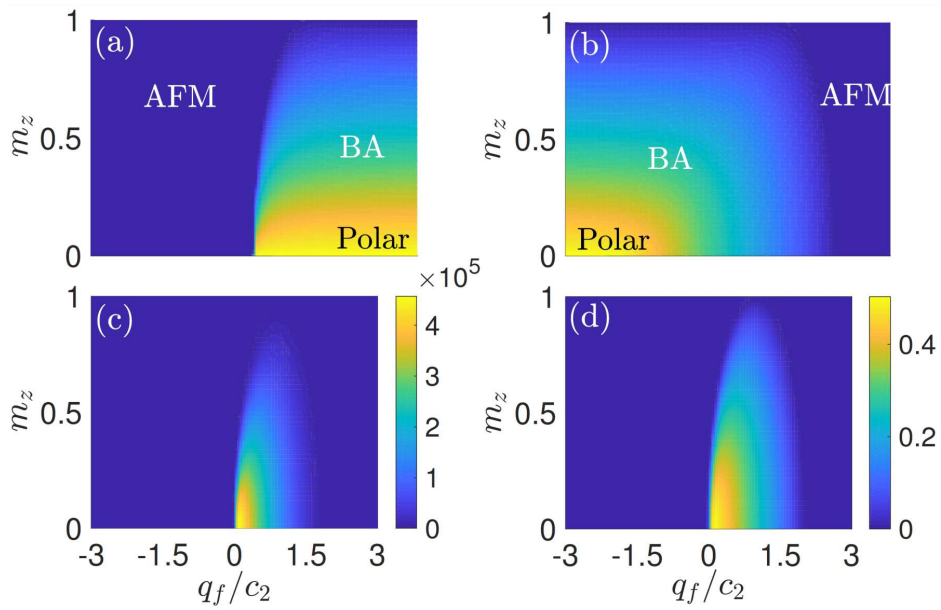

Fig. 5. The fractional population $\mathcal{N}_i$ versus q_f/c_2 and magnetization m_z for (a) the ground state and (b) the highest level. Numerical results of $\Delta\mathcal{N}_0$ (c) and $\mathcal{N}_0$ (d) with respect to q/c_2 and m_z.

then suddenly tune q to q_f and calculate $\Delta\mathcal{N}_m$ and $\mathcal{N}_m$ as time evolves. In Fig. 5c and 5d, we plot $\Delta\mathcal{N}_m$ and $\mathcal{N}_m$ in the plane of m_z and q_f, respectively. We can find that the transition curves of $\Delta\mathcal{N}_m$ and $\mathcal{N}_m$ coincide well with the curves shown in Fig. 5a and b. Thus $\Delta\mathcal{N}_m$ and $\mathcal{N}_m$ can be used to probe the phase transition of the ground state and highest energy level with nonzero magnetization m_z.

4. Conclusions

In summary, we have studied the dynamics of the atomic fluctuation in a spinor condensate and shown that atomic number fluctuations can be used to characterize the DQPTs of the spinor condensate. The dynamical behaviors of the atomic number fluctuations reflect both the ground phase transition between the AFM phase and polar phase and the transition between the polar phase and the BA state for the highest energy level. We show that the generated state by the spin mixing dynamics with $q_f = 0$ exhibits Heisenberg scaling of the metrological sensitivity with N, as quantified by the quantum Fisher information. We further investigate the atomic number fluctuations for nonzero spin magnetization m_z and show that the quantum fluctuation can be used to probe the phase transitions of the ground state and highest level with nonzero m_z.

Acknowledgments

This work was supported by the Natural Science Foundation of Zhejiang Province through grant no. LY22A050002.

References

[1] J. Zhang, G. Pagano, P.W. Hess, A. Kyprianidis, P. Becker, H. Kaplan, A.V. Gorshkov, Z.-X. Gong, C. Monroe, *Nature* **551**, 601 (2017).

[2] P. Jurcevic, H. Shen, P. Hauke, C. Maier, T. Brydges, C. Hempel, B.P. Lanyon, M. Heyl, R. Blatt, C.F. Roos, *Phys. Rev. Lett.* **119**, 080501 (2017).

[3] H. Bernien, S. Schwartz, A. Keesling, H. Levine, A. Omran, H. Pichler, S. Choi, A.S. Zibrov, M. Endres, M. Greiner, V. Vuletić, M.D. Lukin, *Nature* **551**, 579 (2017).

[4] N. Fläschner, D. Vogel, M. Tarnowski, B.S. Rem, D.-S. Lühmann, M. Heyl, J.C. Budich, L. Mathey, K. Sengstock, C. Weitenberg, *Nat. Phys.* **14**, 265 (2018).

[5] W. Sun, C.-R. Yi, B.-Z.Wang, W.-W. Zhang, B.C. Sanders, X.-T. Xu, Z.-Y. Wang, J. Schmiedmayer, Y. Deng, X.-J. Liu, S. Chen, J.-W. Pan, *Phys. Rev. Lett.* **121**, 250403 (2018).

[6] S. Smale, P. He, B.A. Olsen, K.G. Jackson, H. Sharum, S. Trotzky, J. Marino, A.M. Rey, J.H. Thywissen, *Sci. Adv.* **5**, eaax1568 (2019).

[7] P. Cejnar, M. Macek, S. Heinze, J. Jolie, J. Dobeš, *J. Phys. A* **39**, L515 (2006).

[8] M.A. Caprio, P. Cejnar, F. Iachello, *Ann. Phys.* **323**, 1106 (2008).

[9] B. Dietz, F. Iachello, M. Miski-Oglu, N. Pietralla, A. Richter, L. von Smekal, J. Wambach, *Phys. Rev. B* **88**, 104101 (2013).

[10] M. Heyl, *Rep. Prog. Phys.* **81**, 054001 (2018).

[11] A.A. Zvyagin, *Low Temp. Phys.* **42**, 971 (2016).

[12] L.E. Sadler, J.M. Higbie, S.R. Leslie, M. Vengalattore, D.M. Stamper-Kurn, *Nature* **443**, 312315 (2006).

[13] L.S. Leslie, A. Hansen, K.C. Wright, B.M. Deutsch, N.P. Bigelow, *Phys. Rev. Lett.* **103**, 250401 (2009).

[14] J. Choi, W.J. Kwon, Y. Shin, *Phys. Rev. Lett.* **108**, 035301 (2012).

[15] J.-Y. Choi, W.J. Kwon, M. Lee, H. Jeong, K. An, Y.-I. Shin, *New J. Phys.* **14**, 053013 (2012).

[16] L.-Y. Qiu, H.-Y. Liang, Y.-B. Yang, H.-X. Yang, T. Tian, Y. Xu, L.-M. Duan, *Sci. Adv.* **6**, eaba7292 (2020).

[17] S.R. Leslie, J. Guzman, M. Vengalattore, J.D. Sau, M.L. Cohen, D.M. Stamper-Kurn, *Phys. Rev. A* **79**, 043631 (2009).

[18] M. Vengalattore, J. Guzman, S.R. Leslie, F. Serwane, D.M. Stamper-Kurn, *Phys. Rev. A* **81**, 053612 (2010).

[19] J. Kronjäger, C. Becker, P. Soltan-Panahi, K. Bongs, K. Sengstock, *Phys. Rev. Lett.* **105**, 090402 (2010).

[20] J. Guzman, G.-B. Jo, A.N. Wenz, K.W. Murch, C.K. Thomas, D.M. Stamper-Kurn, *Phys. Rev. A* **84**, 063625 (2011).

[21] C.V. Parker, L. Ha, C. Chin, *Nat. Phys.* **9**, 769774 (2013).

[22] E. M. Bookjans, A. Vinit, C. Raman, *Phys. Rev. Lett.* **107**, 195306 (2011).

[23] A. Vinit, E.M. Bookjans, C.A.R. Sá de Melo, C. Raman, *Phys. Rev. Lett.* **110**, 165301 (2013).

[24] T.M. Hoang, M. Anquez, B.A. Robbins, X.Y. Yang, B.J. Land, C.D. Hamley, M.S. Chapman, *Nat. Commun.* **7**, 11233 (2016).

[25] M. Anquez, B.A. Robbins, H.M. Bharath, M. Boguslawski, T.M. Hoang, M.S. Chapman, *Phys. Rev. Lett.* **116**, 155301 (2016).

[26] J.H. Kim, S.W. Seo, Y. Shin, *Phys. Rev. Lett.* **119**, 185302 (2017).

[27] M. Prüfer, P. Kunkel, H. Strobel, S. Lannig, D. Linnemann, C.-M. Schmied, J. Berges, T. Gasenzer, M. K. Oberthaler, *Nature* **563**, 217 (2018).

[28] S. Kang, S.W. Seo, H. Takeuchi, Y. Shin, *Phys. Rev. Lett.* **122**, 095301 (2019).

[29] K. Jiménez-García, A. Invernizzi, B. Evrard, C. Frapolli, J. Dalibard, F. Gerbier, *Nat. Commun.* **10**, 1422 (2019).

[30] Z. Chen, T. Tang, J. Austin, Z. Shaw, L. Zhao, Y. Liu, *Phys. Rev. Lett.* **123**, 113002 (2019).

[31] S. Kang, D. Hong, J.H. Kim, Y. Shin arXiv:1909.00681 (2020).

[32] H.-X. Yang, T. Tian, Y.-B. Yang, L.-Y. Qiu, H.-Y. Liang, A.-J. Chu, C.B. Dag, Y. Xu, Y. Liu, L.-M. Duan, *Phys. Rev. A* **100**, 013622 (2019).

[33] T. Tian, H.-X. Yang, L.-Y. Qiu, H.-Y. Liang, Y.-B. Yang, Y. Xu, L.-M. Duan, *Phys. Rev. Lett.* **124**, 043001 (2020).

[34] A.S. Søensen, K. Mølmer, *Phys. Rev. Lett.* **86**, 4431 (2001).

[35] J.K. Korbicz, J.I. Cirac, M. Lewenstein, *Phys. Rev. Lett.* **95**, 120502 (2005).

[36] J.K. Korbicz, O. Gühne, M. Lewenstein, H. Haffner, C.F. Roos, R. Blatt, *Phys. Rev. A* **74**, 052319 (2006).

[37] A. Sørensen, L.-M. Duan, J. Cirac, P. Zoller, *Nature* **409**, 63 (2001).

[38] G. Tóth, C. Knapp, O. Gühne, H.J. Briegel, *Phys. Rev. A* **79**, 042334 (2009).

[39] L. Pezzé, A. Smerzi, *Phys. Rev. Lett.* **102**, 100401 (2009).

[40] P. Hyllus, L. Pezzé, A. Smerzi, G. Tóth, *Phys. Rev. A* **86**, 012337 (2012).

[41] D. Leibfried, M. Barrett, T. Schaetz, J. Britton, J. Chiaverini, W. Itano, J. Jost, C. Langer, D. Wineland, *Science* **304**, 1476 (2004).

[42] R.J. Lewis-Swan, M.A. Norcia, J.R.K. Cline, J.K. Thompson, A.M. Rey, *Phys. Rev. Lett.* **121**, 070403 (2018).

[43] C. Gross, T. Zibold, E. Nicklas, J. Esteve, M.K. Oberthaler, *Nature* **464**, 1165 (2010).

[44] M.F. Riedel, P. Böhi, Y. Li, T.W. Hänsch, A. Sinatra, P. Treutlein, *Nature* **464**, 1170 (2010).

[45] I.D. Leroux, M.H. Schleier-Smith, V. Vuletić, *Phys. Rev. Lett.* **104**, 073602 (2010).

[46] A. Louchet-Chauvet, J. Appel, J.J. Renema, D. Oblak, N. Kjaergaard, E.S. Polzik, *New J. Phys.* **12**, 065032 (2010).

[47] V. Giovannetti, S. Lloyd, L. Maccone, *Nat. Photon.* **5**, 222 (2011).

[48] C. Lee, J. Huang, H. Deng, H. Dai, J. Xu, *Front. Phys.* **7**, 109 (2012).

[49] R.J. Sewell, M. Koschorreck, M. Napolitano, B. Dubost, N. Behbood, M.W. Mitchell, *Phys. Rev. Lett.* **109**, 253605 (2012).

[50] E. Yukawa, G.J. Milburn, C.A. Holmes, M. Ueda, K. Nemoto, *Phys. Rev. A* **90**, 062132 (2014).

[51] J.G. Bohnet, K.C. Cox, M.A. Norcia, J.M. Weiner, Z. Chen, J.K. Thompson, *Nat. Photon.* **8**, 731 (2014).

[52] D.M. Stamper-Kurn, M.R. Andrews, A.P. Chikkatur, S. Inouye, H.J. Mesner, J. Stenger, W. Ketterle, *Phys. Rev. Lett.* **80**, 2027 (1998).

[53] J. Stenger, S. Inouye, D. M. Stamper-Kurn, H.-J. Miesner, A.P. Chikkatur, W. Ketterle, *Nature* **396**, 345 (1998).

[54] M. Barret, J. Sauer, M.S. Chapman, *Phys. Rev. Lett.* **87**, 010404 (2001).

[55] Y. Kawaguchi, M. Ueda, *Phys. Rep.* **520**, 253 (2012).

[56] D.M. Stamper-Kurn, M. Ueda, *Rev. Mod. Phys.* **85**, 1191 (2013).

[57] L. Zhao, J. Jiang, T. Tang, M. Webb, Y. Liu, *Phys. Rev. A* **89**, 023608 (2014).

[58] Y. Liu, E. Gomez, S.E. Maxwell, L.D. Turner, E. Tiesinga, P.D. Lett, *Phys. Rev. Lett.* **102**, 225301 (2009).

[59] W. Zhang, D.L. Zhou, M.-S. Chang, M.S. Chapman, L. You, *Phys. Rev. A* **72**, 013602 (2005).